A MAC and PHY Cross-Layer Analytical Model for the Goodput and Delay of IEEE 802.11a Networks Operating Under Basic Access and RTS/CTS DCF Schemes

Roger Pierre Fabris Hoefel
University La Salle - Canoas - Brazil
E-mail: roger@unilasalle.edu.br

Abstract — **We have developed a theoretical cross-layer model that allows assessing the goodput and delay of IEEE 802.11 local area networks (WLANs) operating simultaneously under the distributed coordination function (DCF) basic access (BA) and request-to-send/clear-to-send (RTS/CTS) medium access control (MAC) protocols under saturated traffic over correlated fading channels. A comparison between numerical and simulation results is carried out assuming the IEEE 802.11a PHY layer.**

Index Terms— **802.11, Cross-layer, Goodput, Delay, Fading.**

I. INTRODUCTION AND RELATED WORKS

The release of the first IEEE 802.11 standard (that specifies the MAC and the original slower frequency-hopping and direct sequence PHY layers) in 1997 paved the way for a world wide development of a standardized cost-effective scalable technology for WLANs. Since then, intensive research activities have been carried out on analyze, design, implementation, and optimization issues of IEEE 802.11 networks. In 1997, B. P. Crow et al [1] published one of the first papers to explain the IEEE 802.11 specification (with particular emphasis on the MAC layer) and to show simulation results for packetized data and a combination of packetized data and voice over WLANs. In 2000, G. Bianchi [2] proposed an analytical bi-dimensional Markov model to estimate the performance of IEEE 802.11 networks operating under saturated traffic conditions over ideal channels (i.e. only collisions were taken into account and, therefore, the frames were not corrupted due to noise and interference). This Bianchi's model has been recently used as a framework to analyze others IEEE 802.11 technologies, as in [3] where it is proposed an analytical model to assess the performance of quality of service (QoS) schemes for IEEE 802.11 WLANs operating under saturated traffic conditions over ideal channels. In 2002, S. D. Qiao and et al [4] derived an analytical model that takes the non-ideal channel into account on the performance of IEEE802.11a WLANs. However, they assumed an additive white Gaussian noise (AWGN) channel and a simple analytical model to model the MAC layer issues. Therefore, due to the properties of the random multipath radio channel and the use of advanced PHY layer techniques, there was also a necessity to develop an accurate joint MAC and PHY theoretical model to estimate the performance of IEEE 802.11based networks. Hence, based on the methodology proposed by Bianchi in [2], we have developed a cross-layer saturation goodput theoretical model that allows assessing the performance of IEEE 802.11a WLANs over uncorrelated [5] and correlated fading channels [6]. We have also have noticed a lack in the literature on theoretical analyzes of IEEE 802.11 WLANs when both the BA and RTS/CTS access schemes are simultaneously operational, even when it is assumed an ideal PHY layer. Therefore, in the present contribution we have improved our previous theoretical results by: *(1)* developing a MAC and PHY cross-layer model that allows to estimate the goodput and delay of IEEE 802.11a WLANs operating simultaneously under the basic and RTS/CTS access schemes; *(2)* carrying out a unified comparison between the performance of IEEE 802.11a WLANs over uncorrelated and correlated fading channels when both schemes are operational.

The present contribution is organized as follows. In Sections II and III, we briefly present meaningful aspects regarding the IEEE 802.11 MAC and IEEE 802.11a PHY layers, respectively. The analytical results for the goodput and average delay are developed in Sections IV and V, respectively. In Sections VI, we present analytical results to estimate the IEEE 802.11a frame success probability over correlated fading channels. In Section VII, we briefly describe an IEEE 802.11 MAC and PHY layer simulator that have been developed to assess the performance of IEEE 802.11based networks. In Section VIII, we show a meaningful set of IEEE 802.11a analytical and simulation results for the goodput and average delay over distinct environments. Finally, our conclusions are carried out in Section IX.

II. IEEE 802.11 MAC LAYER

The IEEE PHY standards 802.11, 802.11a and 802.11b use the same MAC layer protocols. To accomplish it, a MAC service unit (MSDU) is segmented into a MAC protocol data unit (MPDU) that, on its turn, it is mapped to the physical layer using a standardized physical layer convergence procedure (PLCP). As the IEEE 802.11 MAC protocol is widely known, we only show at Figures 1 and 2 the time diagram for the atomic transmission used by the DCF BA and RTS/CTS mechanisms [7, pp. 57-58]. Notice that DIFS stands for DCF interframe spacing (IFS), PIFS for point coordination IFS, SIFS for short IFS and NAV for network allocation vector.

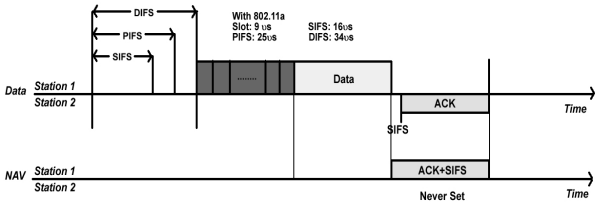

Figure 1. The atomic cycle for the BA scheme.

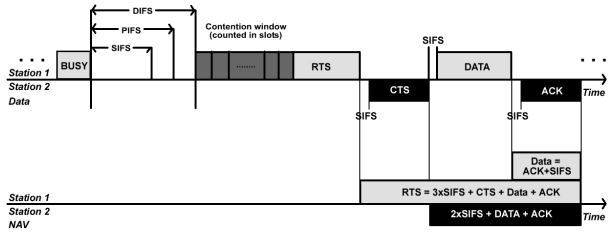

Figure 2. The atomic cycle for the RTS/CTS scheme.

III. IEEE 802.11a PHYSICAL LAYER

The IEEE 802.11a, see Tab. 1, is based on orthogonal frequency division modulation (OFDM) using a total of *52* subcarriers, of which *48* subcarriers carry actual data and *4* subcarriers are pilots used to facilitate coherent detection [8]. The OFDM symbol interval (*tS*) is set to $4\mu s$, and the symbol rate R_s is of *12 Msymbols/sec*.

TABLE I
The IEEE 802.11a PHY modes [4]: *BpS* means *Bytes per Symbol*.

Mode p	*Modulation*	*Code Rate* R_c	*Data Rate*	*BpS*
1	BPSK	1/2	6 Mbps	3
2	BPSK	3/4	9 Mbps	4.5
3	QPSK	1/2	12 Mbps	6
4	QPSK	3/4	18 Mbps	9
5	16-QAM	1/2	24 Mbps	12
6	16-QAM	3/4	36 Mbps	18
7	64-QAM	2/3	48 Mbps	24
8	64-QAM	3/4	54 Mbps	27

Considering the IEEE 802.11a convolutional codes generator polynomials, $g_0=(133)_8$ and $g_1=(171)_8$, of rate $R_c=1/2$ and constrain length $K=7$, then the union bound on the probability of decoding error is given by [9]

$$P_e(\gamma_b,p) < 11P_{10}(\gamma_b,p)+38P_{12}(\gamma_b,p)+193P_{14}(\gamma_b,p)+\cdots, \quad (1)$$

where the notation emphasizes the dependence of P_d with the received signal-to-interference-plus-noise (SINR) per bit γ_b, and the PHY mode p.

The union bound on the probability of decoding error for the higher code rates of 2/3 and 3/4 (which are obtained by puncturing the original rate-1/2 code), are given by (2) and (3), respectively [10].

$$P_e(\gamma_b,p) < P_6(\gamma_b,p)+16P_7(\gamma_b,p)+48P_8(\gamma_b,p)+\cdots \quad (2)$$

$$P_e(\gamma_b,p) < 8P_5(\gamma_b,p)+31P_6(\gamma_b,p)+160P_7(\gamma_b,p)+\cdots \quad (3)$$

Assuming that the convolutional forward error correcting code (FEC) is decoded using hard-decision Viterbi decoding, then (4-5) model the probability of selecting incorrectly a path when the Hamming distance d is even and odd, respectively. The average bit error rate (BER) for the PHY mode p is denoted by ρ_p.

$$P_d(\gamma_b,p)=\frac{1}{2}\binom{d}{d/2}\rho_p^{d/2}(1-\rho_p)^{d/2}+\sum_{k=d/2+1}^{d}\binom{d}{k}\rho_p^k(1-\rho_p)^{d-k}. \quad (4)$$

$$P_d(\gamma_b,p)=\sum_{k=(d+1)/2}^{d}\binom{d}{k}\rho_p^k(1-\rho_p)^{d-k}. \quad (5)$$

The number of octets of the PHY layer protocol data unit (PDU) for the RTS frame is given by

$$N_{rts}=N_{pre}+N_{srv}+l_{rts}+N_{tail}=3+\frac{16}{8}+20+\frac{6}{8}, \quad (6)$$

where N_{pre}, N_{srv} and N_{tail} denote the number of octets of the preamble, service and tail fields, respectively. The number of octets used to carry the "logical control information" sent by the RTS, CTS and ACK control frames is labelled by l_{rts}, l_{cts} and l_{ack}, respectively. Notice that 6 tail bits, N_{tail}, are used to flush the convolutional code to the "zero state".

The number of octets of the PPDU that transport the CTS and ACK control frame is given by

$$N_{cts}=N_{ack}=N_{pre}+N_{srv}+l+N_{tail}=3+\frac{16}{8}+14+\frac{6}{8}, \quad (7)$$

where $l=l_{cts}=l_{ack}=14$ *octets*.

The MAC PPDU length is given by

$$N_{mp}=N_{pre}+N_{srv}+N_{mh}+l_{pl}+N_{tail}=3+\frac{16}{8}+34+l_{pl}+\frac{6}{8}, \quad (8)$$

where the MPDU header and the cyclic redundant checking (CRC) fields have together a length of *34* bytes ($N_{mh}=34$) [7, pp. 46]. l_{pl} labels the MPDU payload.

The RTS and CTS control frames must be transmitted using the basic service set (BSS) basic rate (i.e. PHY modes 1, 3 and 5). The ACK control frames must be transmitted using the BSS basic rate that is less than or equal to the rate of the data frame it is acknowledging.

The length of RTS, CTS and ACK control frames are given by (9-11), respectively. The PHY layer convergence procedure (PLCP) preamble duration, *tPCLP_Pre*, is equal to *16* μs. The PCLP header is always transmitted using PHY 1 and its duration, *tPCLP_SIG*, is equal to $4\mu s$ [4].

$$T_{rts}(p_{rts})=tPCLP\_Pre+tPCLP\_SIG+\left\lceil\frac{l_{rts}+(16+6)/8}{BpS(p_{rts})}\right\rceil\cdot tS. \quad (9)$$

$$T_{cts}(p_{cts}) = tPCLP\_Pre + tPCLP\_SIG + \left\lceil \frac{l_{cts} + (16+6)/8}{BpS(p_{cts})} \right\rceil \cdot tS \,. \quad (10)$$

$$T_{ack}(p_{ack}) = tPCLP\_Pre + tPCLP\_SIG + \left\lceil \frac{l_{ack} + (16+6)/8}{BpS(p_{ack})} \right\rceil \cdot tS. \quad (11)$$

The time period spent to transmit a MPDU with a payload of l_{pl} octets over the IEEE 802.11a using the PHY mode p_{mp} is given by.

$$T_{mp}(p_{mp}) = tPCLP\_Pre + tPCLP\_SIG + \left\lceil \frac{N_{pl} + 34 + (16+6)/8}{BpS(p_{mp})} \right\rceil \cdot tS \,. \quad (12)$$

IV. Analytical Results: Saturation Goodput

Fig. 3 shows a discrete bi-dimensional Markov chain $(s_i(t), b_i(t))$ for a IEEE 802.11 STA. The present analytical modelling, that models the backoff window size and the non-ideal channel conditions, assumes that:

1. there is a fixed number of n STAs that operate in saturation conditions, i.e. each STA has a MPDU to transmit after finishing each successful transmission;
2. a MPDU frame is transmitted using the BA and RTS/CTS schemes with probability P_{ba} and P_{rts}, respectively;
3. $s_i(t)$ is a stochastic process that models the *ith backoff stage* at time t, where $i \in (0,\cdots,m)$;
4. $b_i(t)$ is a stochastic process that models the backoff time counter for *the backoff stage i* at time t;
5. the window size at backoff stage i is $W_i = 2^i W$, where W is the MAC contention window (CW) size parameter, CW_{min}. The maximum window size for the *STA* is denoted as $W_m = CW_{max} - 1 = 2^m W - 1$;
6. the MPDUs transmitted by the STAs collide with a constant and independent conditional collision probability p;
7. the capture effect is neglected as such as the lost of frames due to collisions is independent of the lost of frames due to noise and interference;
8. the post backoff procedure [3] is not taken into account.

The probability that a transmitted MPDU is successful depends upon the following events: *(1)* no collision and successful transmission using the BA scheme; *(2)* no collision and successful transmission using the RTS/CTS access scheme. Thus,

$$P_s = (1-p)\cdot\left\{P_{ba}\cdot(S_{mp}\cdot S_{ack}) + P_{rts}\cdot(S_{rts}\cdot S_{cts}\cdot S_{mp}\cdot S_{ack})\right\}, \quad (13)$$

where S_{cts}, S_{rts} and S_{ack} denote, respectively, the probability that the RTS, CTS and ACK control frames be transmitted with success. S_{mp} denotes the probability the transmission of a MPDU frame is successful.

Eq. (14) and (15) model the probability that a MPDU is transmitted using the BA and RTS/CTS schemes, respectively. Notice that these probabilities depend upon the MAC payload length l_{pl} and the *RTSThreshold* defined at the Management Information Base (MIB).

$$P_{ba} = P\{l_{pl} < RTSThreshold\}. \quad (14)$$

$$P_{rts} = P\{l_{pl} \geq RTSTheshold\}. \quad (15)$$

Eq. (16) details the events that cause an unsuccessful MPDU transmission: *(1)* collision; *(2)* no collision, but a corrupted frame on the basis access scheme (see 17); *(3)* no collision, but a corrupted frame on the RTS/CTS access scheme (see 18).

$$P_f = p + (1-p)\cdot(P_{ba}\cdot P_{f,ba} + P_{rts}\cdot P_{f,rts}). \quad (16)$$

$$P_{f,ba} = (1 - S_{mp}) + S_{mp}\cdot(1 - S_{ack}) = 1 - S_{mp}\cdot S_{ack} \quad (17)$$

$$P_{f,rts} = \left[\begin{array}{l}(1 - S_{rts}) + S_{rts}\cdot(1 - S_{cts}) + \\ S_{rts}\cdot S_{cts}\cdot(1 - S_{mp}) + S_{rts}\cdot S_{cts}\cdot S_{mp}\cdot(1 - S_{ack})\end{array}\right] = 1 - S_{rts}\cdot S_{cts}\cdot S_{mp}\cdot S_{ack} \quad (18)$$

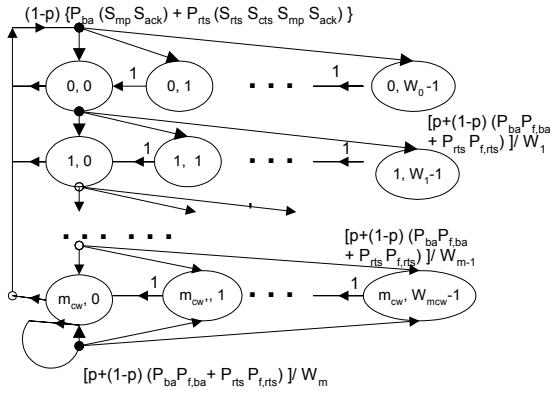

Figure 3. Bi-dimensional Markov chain (s(t),b(t)) model for the backoff window size and a non-ideal channel.

A. Packet Transmission Probability

Equations (19) to (22) model the null one-step transition probabilities of the bi-dimensional Markov chain depicted at Fig. 3, where it is used the notation $P\{i_1,k_1/i_0,k_o\} = P\{s(t+1)=i_1, b(t+1)=k_1 \mid s(t)=i_o, b(t)=k_o\}$.

The decreasing of the backoff timer at the beginning at each slot time of size σ is modeled as

$$P\{i,k \mid i,k+1\} = 1 \quad for\ k \in (0, W_i - 2)\ and\ i \in (0,m). \quad (19)$$

Eq. (20) takes into account that a new PHY layer PDU (PPDU) starts at the backoff stage 0 and that the backoff is uniformly distributed into the range $(0, W_0\text{-}1)$ after a successful PPDU transmission.

$$P\{0,k \mid i,0\} = [1-p]\cdot\left[\begin{array}{l}P_{ba}\cdot(S_{mp}\cdot S_{ack}) + \\ P_{rts}\cdot(S_{rts}\cdot S_{cts}\cdot S_{mp}\cdot S_{ack})\end{array}\right]/W_0 \quad for\ k \in (0, W_0 - 1)\ and\ i \in (0,m). \quad (20)$$

The property that a new backoff value is uniformly chosen in the range $(0,W_i)$ after an unsuccessful transmission at the backoff stage $i\text{-}1$ can be modeled as

$$P\{i,k \mid i-1,0\} = \{p + [1-p]\cdot\left[\begin{array}{l}P_{ba}\cdot(1 - S_{mp}\cdot S_{ack}) + \\ P_{rts}\cdot(1 - S_{rts}\cdot S_{cts}\cdot S_{mp}\cdot S_{ack})\end{array}\right]\}/W_i. \quad (21)$$

Eq. (22) models the fact that the backoff is not increased in subsequent frame transmissions once the backoff stage has reached the value m.

$$P\{m,k \mid m,0\} = \{p + [1-p] \cdot \begin{bmatrix} P_{ba} \cdot (1 - S_{mp} \cdot S_{ack}) + \\ P_{rts} \cdot (1 - S_{rts} \cdot S_{cts} \cdot S_{mp} \cdot S_{ack}) \end{bmatrix}\} / W_m \cdot \quad (22)$$

The MPDU transmission occurs when the backoff timer counter is equal to zero. Therefore, using an algebraic procedure similar to that one developed in [5] we can show that the probability that a STA transmits in a randomly chosen slot time is given by (23), where, the stationary probability of a given STA be in the time slot 0 for first contention window is given by (24). The average frame success transmission probability is denoted by S, as indicated by (25).

$$\tau = \sum_{i=0}^{m} b_{i,0} = \frac{b_{0,0}}{(1-p) \cdot [P_{ba} \cdot (S_{mp} \cdot S_{ack}) + P_{rts} \cdot (S_{rts} \cdot S_{cts} \cdot S_{mp} \cdot S_{ack})]} \cdot \quad (23)$$

$$b_{0,0} = \frac{2 \cdot (1-p) \cdot S \cdot [1 + 2 \cdot S \cdot (p-1)]}{1 + 2^m W \cdot [1 + (-1+p) \cdot S]^m + (-1+p) \cdot S \cdot \{2 + W + 2^m W \cdot [1 + (-1+p) \cdot S]^m\}} \quad (24)$$

$$S = P_{ba} \cdot (S_{mp} \cdot S_{ack}) + P_{rts} \cdot (S_{rts} \cdot S_{cts} \cdot S_{mp} \cdot S_{ack}). \quad (25)$$

For an ideal channel (i.e. $S_{rts}=S_{cts}= S_{mp}= S_{ack} =1$), Eq. (24) resumes to (26), which agrees with (6) of [2].

$$b_{0,0} = \frac{2(1-2p) \cdot (1-p)}{(1-2p) \cdot (W+1) + pW \cdot (1-(2p)^m)} \cdot \quad (26)$$

Each STA transmits with probability τ. Therefore, the conditional probability that a transmitted PPDU encounters a collision in a given slot time can be stated as

$$p = 1 - (1-\tau)^{n-1} \cdot \quad (27)$$

The nonlinear system represented by (23) and (27) can be solved using numerical techniques in order to estimate the transmission probability τ and the conditional collision probability p.

B. Goodput

The goodput (net throughput) in bits per second (bps) can be modeled as the ratio of the payload bits transmitted with success to the average cycle time, i.e.

$$G_{bps} = \frac{P_{ba} \cdot \overline{N}_{ba} + P_{rts} \cdot \overline{N}_{rts}}{P_{ba} \cdot \overline{T}_{ba} + P_{rts} \cdot \overline{T}_{rts}} \cdot \quad (28)$$

The average number of payload bits transmitted with success for the BA and RTS/CTS schemes are given by (29) and (30), respectively. The number of payload octets when is used the BA and RTS/CTS schemes are denoted by $l_{pl,ba}$ and $l_{pl,rts}$, respectively.

$$\overline{N}_{ba} = 8 \cdot l_{pl,ba} \cdot P_s \cdot P_{tr} \cdot S_{mp} \cdot S_{ack} \cdot \quad (29)$$

$$\overline{N}_{rts} = 8 \cdot l_{pl,rts} \cdot P_s \cdot P_{tr} \cdot S_{rts} \cdot S_{cts} \cdot S_{mp} \cdot S_{ack} \cdot \quad (30)$$

The probability that there is no collision on the channel conditioned to the fact that at least one STA transmits is given by

$$P_s = \frac{\binom{n}{1} \cdot \tau \cdot (1-\tau)^{n-1}}{P_{tr}} = \frac{n \cdot \tau \cdot (1-\tau)^{n-1}}{P_{tr}} = \frac{n \cdot \tau \cdot (1-\tau)^{n-1}}{1-(1-\tau)^n} \cdot \quad (31)$$

where P_{tr} is the probability that there is at least one transmission in the considered slot time.

The average cycle time for the basic access and RTS/CTS scheme is given by (32) and (33), respectively.

$$\overline{T}_{ba} = \overline{B}_{s,ba} + \overline{B}_{f1,ba} + \overline{B}_{f2,ba} + \overline{B}_{f3,ba} + \overline{I} \cdot \quad (32)$$

$$\overline{T}_{rts} = \overline{B}_{s,rts} + \overline{B}_{f1,rts} + \overline{B}_{f2,rts,} + \overline{B}_{f3,rts} + B_{f4,rts} + B_{f5,rts} + \overline{I} \cdot \quad (33)$$

For the BA scheme, the average busy time when the atomic positive ACK basic access transmission is successful is given by

$$\overline{B}_{s,ba} = P_s \cdot P_{tr} \cdot S_{mp} \cdot S_{mac} \cdot \begin{pmatrix} DIFS + T_{mp}(p_{mp}) + a + \\ SIFS + T_{ack}(p_{ack}) + a \end{pmatrix}. \quad (34)$$

where a is the propagation delay. $T_{mp}(p_{mp})$ is the time period necessary to transmit a MPDU when it is used the PHY mode p_{mp} (see 12). $T_{ack}(p_{ack})$ is the time period spent to transmit a positive ACK control frame using the PHY mode p_{ack} (see 11).

The average busy time when the transmission is successful using the RTS/CTS scheme is given by

$$\overline{B}_s = P_s \cdot P_{tr} \cdot S_{rts} \cdot S_{cts} \cdot S_{mp} \cdot S_{mac} \cdot [DIFS + T_{rts}(p_{rts}) + a + SIFS + T_{cts}(p_{cts}) + a + SIFS + T_{mp}(p_{mp}) + a + SIFS + T_{ack}(p_{ack}) + a] \quad (35)$$

where $T_{rts}(p_{rts})$ and $T_{cts}(p_{cts})$ denote the time necessary to transmit the RTS and CTS control frames when it is used the PHY mode p_{rts} and p_{cts}, respectively (see 9 and 10).

$\overline{B}_{f1,ba}$ models the average amount of time that the channel is busy due to collisions of a MPDU frames when it used the BA scheme (see 36). However, for the RTS/CTS MAC scheme the waste time occurs due to RTS control frame collisions, as modeled by (37).

$$\overline{B}_{f1,ba} = P_{tr} \cdot (1 - P_s) \cdot (DIFS + T_{mp}(p_{mp}) + a) \cdot \quad (36)$$

$$\overline{B}_{f1,rts} = P_{tr} \cdot (1 - P_s) \cdot (DIFS + T_{rts}(p_{rts}) + a) \cdot \quad (37)$$

$\overline{B}_{f2,ba}$ and $\overline{B}_{f3,ba}$ model the average lost time due to an unsuccessful transmissions due to noise and interference of data and ACK frames, respectively, when it is used the BA scheme.

$$\overline{B}_{f2,ba} = P_{tr} \cdot P_s \cdot (1 - S_{mp}) \cdot (DIFS + T_{mp}(p_{mp}) + a). \quad (38)$$

$$\overline{B}_{f3,ba} = P_{tr} \cdot P_s \cdot S_{mp} \cdot (1 - S_{ack}) \cdot \begin{pmatrix} DIFS + T_{mp}(p_{mp}) + a + \\ SIFS + T_{ack}(p_{ack}) + a \end{pmatrix}. \quad (39)$$

$\overline{B}_{f2,rts}$, $\overline{B}_{f3,rts}$, $\overline{B}_{f4,rts}$ and $\overline{B}_{f5,rts}$ model the average time that the channel is busy with unsuccessful transmissions due to noise and interference, of RTS, CTS, data and ACK frames, respectively, when it is used

the RTS/CTS access scheme. Finally, the average time that a slot time is idle is given by (39), where σ is the slot time length.

$$\overline{B}_{f\,2,rts} = P_{tr}\cdot P_s\cdot(1-S_{rts})\cdot\left[DIFS + T_{rts}(p_{rts}) + a\right]. \quad (40)$$

$$\overline{B}_{f\,3,rts} = P_{tr}\cdot P_s\cdot S_{rts}\cdot(1-S_{cts})\cdot\begin{bmatrix} DIFS+T_{rts}(p_{rts})+a+\\ SIFS+T_{cts}(p_{cts})+a\end{bmatrix}. \quad (41)$$

$$\overline{B}_{f\,4,rts} = P_{tr}\cdot P_s\cdot S_{rts}\cdot S_{cts}\cdot(1-S_{mp})\cdot\left[DIFS + T_{rts}(p_{rts}) + a + SIFS + T_{cts}(p_{cts}) + a + SIFS + T_{mp}(p_{mp}) + a\right]. \quad (42)$$

$$\overline{B}_{f\,5,rts} = P_{tr}\cdot P_s\cdot S_{rts}\cdot S_{mp}\cdot(1-S_{ack})\cdot\left[DIFS + T_{rts}(p_{rts}) + a + SIFS + T_{rcs}(p_{cts}) + a + SIFS + T_{mp}(p_{mp}) + a + SIFS + T_{ack}(p_{ack}) + a\right]. \quad (43)$$

$$\overline{I} = (1-P_{tr})\cdot\sigma\ . \quad (44)$$

V. Analytical Results: Average Delay

The average delay between the time that a MPDU arrived at the queue until the time that an positive ACK for this MPDU is received can be modeled as the average number of cycle times necessary to accomplish a successful MPDU transmission, as modeled by (45). The average cycle time for the BA and RTS/CTS schemes is given by (32) and (33), respectively. The average number of time slots spent for a successful transmission is given by (46), where the average probability that an atomic transmission is not successful, P_f, is given by (16).

$$\overline{D} = \overline{P}\cdot\left\{P_{ba}\cdot\overline{T}_{ba} + P_{rts}\cdot\overline{T}_{rts}\right\}. \quad (45)$$

$$\overline{P} = \sum_{i=0}^{m-1}\left[(P_f)^i\frac{W_i}{2}\right] + \sum_{i=m}^{\infty}\left[(P_f)^i\cdot\frac{W_m}{2}\right]. \quad (46)$$

VI. Analytical Results: Frame Success Probability over Block Fading Channels

In this Section, we assume that the fading is correlated at each atomic cycle (see Fig. 1 and 2) and uncorrelated among distinct atomic cycles.

Assuming hard decision Viterbi decoding, then the upper bound for a successful frame transmission over an uncorrelated fading channel can be estimated by (47) for a frame with l octets [11]. For a block-fading channel, this upper bound must be modified to take into account the channel memory. Eq. (48) estimates the average probability that a hard decision Viterbi decoder decodes successfully a frame with *l octets* transmitted using the PHY mode p when the mulitpath fading with average SINR per bit γ_b remains the same during the whole frame transmission. Notice that $p(\gamma_b)$ is the probability distribution function (pdf) of the SINR per bit at the Viterbi decoder input and γ_{inf} is chosen to satisfy the inequality (49).

$$S(l,\gamma_b,p) < \left[1-P_e(\gamma_b,p)\right]^{8l} \quad (47)$$

$$S(l,\gamma_b,p) < \int_{\gamma_{inf}}^{\infty}\left[1-Pe(\gamma_b,p)\right]^{8l}p(\gamma_b)d\gamma_b \quad (48)$$

$$1-Pe(\gamma_{inf},p) \le 1\ . \quad (49)$$

We have assumed a flat fading Nakagami-m channel [12, pp. 47]. Therefore, considering a maximum ratio combining (MRC) receiver matched with the channel diversity and that the same average power is received at each diversity branch, then pdf of the SINR per bit at the Viterbi decoder input is of gamma kind [5], i.e.

$$p(\gamma_b) = \frac{1}{\Gamma(L\,m_n)}\left(\frac{m_n}{\overline{\gamma}_b}\right)^{L\,m_n}(\gamma_b)^{L\,m_n-1}\exp\left(-\frac{m_n\,\gamma_b}{\overline{\gamma}_b}\right) \quad if\ \gamma_b>0,\ m_n\ge 0.5, \quad (50)$$

where m_n is the fading figure, $\overline{\gamma}_b$ is the average SINR per bit at the at Viterbi decoder input and L is the number of independent diversity branches. Notice that $m_n=1$ models a Rayleigh channel.

A. PHY Mode 1 (BPSK@6Mbps)

For the PHY mode 1, the union bound on the decoding error can be estimated using (1) and (4), where the average BER ρ_p is given by (51) with code rate $R_c=1/2$. $Q(x)$ is the complementary Gaussian cumulative distribution function [12, pp. 269].

$$\rho_1 = Q\left(\sqrt{2\gamma_b R_c}\right). \quad (51)$$

Since all frames are transmitted using the PHY mode 1, then S_{rts}, S_{cts}, S_{mp} and S_{ack} can be estimated using (52-58) with $p=1$.

$$S_{rts}(p_{rts}) = S(N_{rts},\gamma_b,p_{rts});\quad (52)$$

$$S_{cts}(p_{cts}) = P\{CTS\ is\ \ ack\ /\ RTS\ was\ ack\};\quad (53)$$

$$S_{cts}(p_{cts}) = \frac{S(N_{rts}+N_{cts},\gamma_b,p_{cts})}{S_{rts}(p_{rts})};\quad (54)$$

$$S_{mp}(p_{mp}) = P\{\ MPDU\ is\ correct\ /\ RTS, CTS\ were\ correct\};\quad (55)$$

$$S_{mp}(p_{mp}) = \frac{S(N_{rts}+N_{cts}+N_{mp},\gamma_b,p_{mp})}{S_{rts}(p_{rts})\cdot S_{cts}(p_{cts})};\quad (56)$$

$$S_{ack}(p_{ack}) = P\{\ ACK\ is\ correct\ /\ RTS, CTS, MPDU\ were\ correct\};\quad (57)$$

$$S_{ack}(p_{ack}) = \frac{S(N_{rts}+N_{cts}+N_{mp}+N_{ack},\gamma_b,p_{ack})}{S_{rts}(p_{rts})\cdot S_{cts}(p_{cts})\cdot S_{mp}(p_{mp})}.\quad (58)$$

B. PHY Mode 2 (BPSK@9Mbps)

When the MPDU is transmitted using the PHY mode 2, then all control frames are transmitted using the PHY mode 1. Thus, the S_{rts} and S_{cts} are still given by (52) and (54), respectively, with $p=1$. The union bound on the decoding error can be estimated using (3) and (5), where ρ_p is given by (51) with $R_c=3/4$. The probability that the MPDU is transmitted with success can be stated as

$$S_{mp}(2) \cong \frac{S(36.75+N_{mp},\gamma_b,2)}{S_{rts}(1)S_{cts}(1)} = \frac{S(36.75+N_{mp},\gamma_b,2)}{S(N_{rts}+N_{cts},\gamma_b,1)} \quad (59)$$

Notice that the 3 octets of the preamble were not taken into account in (59) since they are transmitted using the

PHY mode 1 (i.e. a more robust signaling scheme). We also have used the following approximation:

$$P\{MPDU\,is\,ack/\,RTS\,and\,CTS\,were ack\} = \frac{P\{MPDU,RTS,CTS\}}{P\{RTS,CTS\}} \approx \frac{P\{MPDU\}}{P\{RTS,CTS\}} \quad (60)$$

since $N_{mp}>>(N_{rts}+N_{cts})$, and the MPDU is transmitted using the PHY mode 2 (i.e. a signaling scheme with lesser immunity to noise and interference than the signaling scheme used to transmit the control frames).

The ACK control frame is transmitted using the PHY mode 1, while the MPDU is transmitted using the PHY mode 2 (i.e. a signaling scheme more suitable to the decoding errors). Thus, the ACK control frame success probability can be approximated by (61) for block fading channels. Notice that, usually, $N_{ack}<<N_{mp}$.

$$S_{ack}(p) = P\{ACK\ is\ ack\,/\,RTS, CTS\ and\ MPDU\ were\ ack) \cong 1. \quad (61)$$

C. PHY Mode 3(QPSK@12Mbps)

In this case all control and data frames are transmitted using the PHY mode 3. Therefore, S_{rts} and S_{cts} are given by (52) and (54), respectively, with $p=3$. Correspondingly, S_{md} and S_{ack} are given by (56) and (58), respectively, with $p=3$. The union bound on the decoding error can be estimated using (1) and (4), where ρ_p is given by (51) with $R_c=1/2$ for coherent demodulation [12].

D. PHY Mode 4 (QPSK@18Mbps)

Here, all the control frames are transmitted using the PHY mode 3 and the MPDU is transmitted using the PHY mode 4. Consequently, S_{rts} and S_{cts} are given by (52) and (54), respectively, with $p=3$. Using similar reasoning developed for PHY mode 2, then S_{md} is given by (62) and S_{ack} is given by (61). The union bound on the decoding error can be estimated using (3) and (5), where ρ_p given by (51) with $R_c=3/4$ for coherent demodulation [12].

$$S_{mpd}(4) \cong \frac{S(36.75+N_{mpd},\gamma_b,4)}{S_{rts}(3)S_{cts}(3)} = \frac{S(36.75+N_{mpd},\gamma_b,4)}{S(N_{rts}+N_{cts},\gamma_b,3)}. \quad (62)$$

E. PHY Mode 5 (16QAM@24Mbps)

In this case all control and data frames are transmitted using the PHY mode 5. Therefore, S_{rts} and S_{cts} are given by (52) and (54), respectively, with $p=5$. Correspondingly, S_{md} and S_{ack} are given by (56) and (58) with $p=5$. The union bound on the decoding error can be estimated using (1) and (4). ρ_p for QAM signaling is given by (63) with $M=16$ and $R_c=1/2$ [13].

$$\rho_p = \frac{\sqrt{M}-1}{\sqrt{M}\log_2\sqrt{M}} erfc\left(\sqrt{\frac{2\log_2 M\cdot\gamma_b\cdot R_c}{2(M-1)}}\right) + \frac{\sqrt{M}-2}{\sqrt{M}\log_2\sqrt{M}} erfc\left(\sqrt{\frac{3\log_2 M\cdot\gamma_b\cdot R_c}{2(M-1)}}\right). \quad (63)$$

F. PHY Mode 6 (16QAM@36Mbps), PHY Mode 7 (64QAM@48Mbps) and PHY Mode 8 (64QAM@64Mbps)

For all these PHY modes the control frames are transmitted using the PHY mode 5 and the MPDU is transmitted using the PHY modes 6, 7, or 8. Thus, the S_{rts} and S_{cts} are still given by (52) and (54) with $p=5$. The S_{md} is given by

$$S_{mpd}(p) \cong \frac{S(36.75+N_{mpd},\gamma_b,p)}{S_{rts}(5)S_{cts}(5)} = \frac{S(36.75+N_{mpd},\gamma_b,p)}{S(N_{rts}+N_{cts},\gamma_b,5)}. \quad (64)$$

where $p=6$, 7 and 8. The S_{ack} can be estimated by (61) since the control frames are transmitted using 16QAM with $R_c=1/2$ while the MPDU is transmitted using 16QAM with $R_c=3/4$ (PHY 6), 64QAM with $R_c=2/3$ (PHY 7) or 64QAM with $R_c=3/4$ (PHY 8).

VII. JOINT MAC AND PHY LAYERS SIMULATOR

The C^{++} IEEE 802.11 joint MAC and PHY layers simulator has the following main characteristics:

- It implements an ad hoc IEEE 802.11a WLAN.
- It implements the MAC state machine that fulfills the IEEE 802.11 DCF BA and RTS/CTS schemes.
- The OFDM PHY layer is implemented assuming perfect synchronism. The PHY layer signal processing algorithms implements the maximum-likelihood hard decision detection for the PHY mode 1 to PHY mode 8.
- The convolutional hard-decision decoding is implemented using a semi-analytic approach as follows. The short-term average BER is estimated at a frame basis using on-line statistics collected at the demodulator output. Then the average BER is used in (1-5) to estimate the probability that the hard decision Viterbi decoding algorithm produces a decoding error.
- It is assumed the IEEE 802.11a PHY layer parameters [7, pp. 279]: *slot time* $\sigma=9\mu S$, $SIFS=16\mu s$, $DIFS=34\mu s$, $CW_{min}=16$, $CW_{max}=1023$, $m=6$. The propagation delay a is set *to* $1\mu.s$.
- The correlated fading (tantamount for block fading) is generated using the Jakes' model with carrier frequency of 5.5 GHz and velocity of 3 km/h [14].
- It is assumed a confidence interval of *98%*.

VIII. ANALYTICAL AND SIMULATION RESULTS

In this section, assuming correlated and uncorrelated flat fading Rayleigh channels, we shall show simulation and analytical results for the following system configurations: *(1)* IEEE 802.11a networks operating only under the RTS/CTS access scheme: $P_{ba}=0$ and $P_{rts}=1$ in (13) and subsequent equations; (2) IEEE 802.11a networks operating only under the BA mode: $P_{ba}=1$ and $P_{rts}=0$; (3) joint operation of BA and RTS/CTS schemes.

A Single Operation of RTS/CTS Access Scheme Over Correlated Fading Channels

In this subsection, we assume an uncorrelated flat fading Rayleigh channel, $P_{ba}=0$, $P_{rts}=1$. The MAC

payload l_{pl} is set to *1023 octets*.

Fig. 4 compares the goodput as a function of the SINR per bit for a system without spatial diversity (L=1). First, we emphasize a good agreement between analytical andsimulation results. Second, we can conclude that the *PHY mode 3* (QPSK with R_c=1/2) and *PHY mode 4* (QPSK with R_c=3/4) allows, respectively, a superior performance in relation to that one obtained with the *PHY mode 1* (BPSK with R_c=1/2) and *PHY mode 2* (BPSK with R_c=3/4), since the QPSK signalling has a better spectral efficiency when it is implemented coherent demodulation. Fig. 5 shows a reasonable agreement between numerical and simulation results for the average MPDU delay.

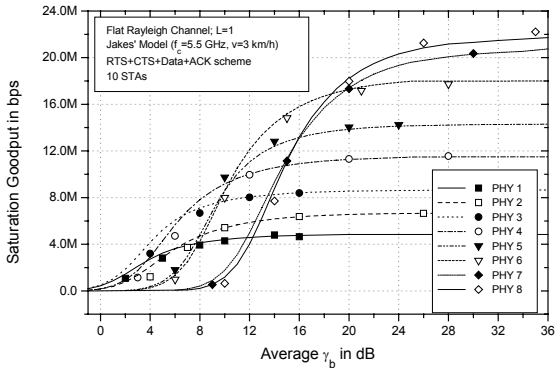

Figure 4. Comparison between analytical (straight lines) and simulation (marks) results for the goodput in bps over a correlated fading channel.

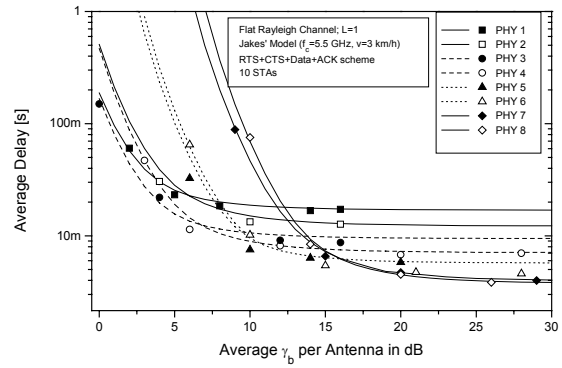

Figure 5. Comparison between analytical (straight lines) and simulation (marks) results for the delay over a correlated fading channel. L=1.

B Comparison of the Performance of RTS/CTS Scheme Over Correlated and Uncorrelated Fading Channels

In this subsection, we assume that the MAC payloads of *1023 octets* are transmitted by the RTS/CTS scheme. Analytical results for uncorrelated fading channels can be found in [5].

Fig. 6 shows that for temporally uncorrelated flat fading Rayleigh channel there is a well-defined short range of SINR per bit where the system performance is acceptable. On the other hand, when the fading is strongly correlated there is a wide and smooth variation of the goodput with SINR per bit. Fig. 6 also shows that the spatial diversity (assumed uncorrelated at each diversity branch) provides a greater gain in the required SINR per bit, γ_b, on environments where the fading is temporally uncorrelated. However, the diversity gain is also substantial on environments where the fading is both temporally and frequency correlated.

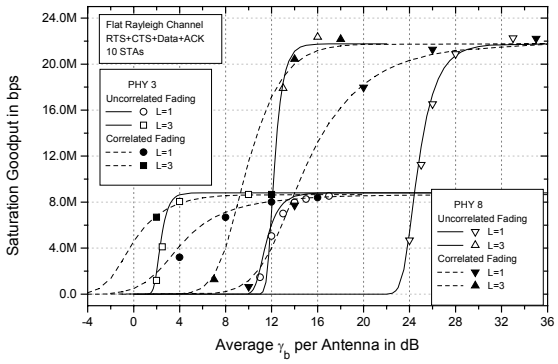

Figure 6. Comparison between analytical (straight lines) and simulation (marks) results for the average goodput.

Hereafter, we shall present results for IEEE 802.11a networks operating simultaneously under the BA and RTS/CTS access schemes. It is generated MAC payloads of *255* and *1023* octets with equal probability (i.e. $P_{ba}=P_{rts}=0.5$). The *RTSThreshold* is set to *256* octets

C Joint Operation of BA and RTS/CTS Access Schemes Over Correlated Fading Channels

In spite of the complexity of the MAC and PHY layers, we can verify a good agreement between analytical and simulation results for the goodput (Fig. 7) and delay (Fig. 8) for the joint operation of BA and RTS/CTS schemes over correlated flat fading Rayleigh channels.

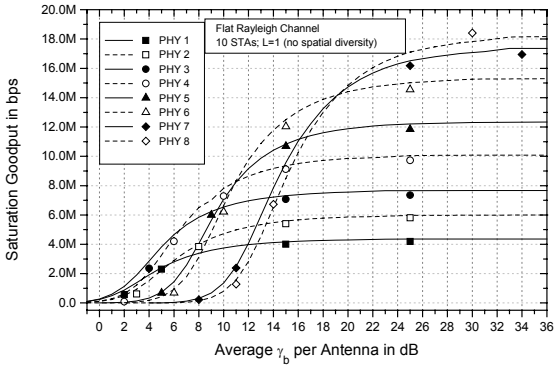

Figure 7. Goodput in bps versus the average SINR per bit.

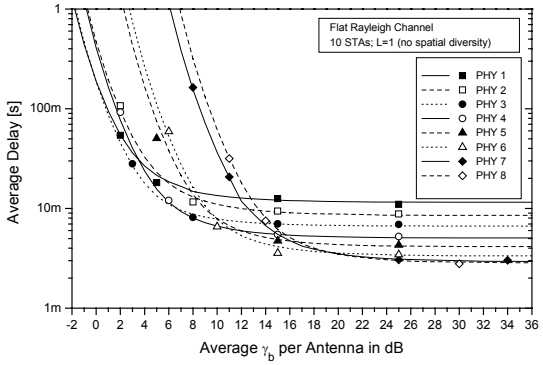

Figure 8. Average delay in seconds versus the average SINR per bit.

D Joint Operation of BA and RTS/CTS Access Schemes Over Uncorrelated Fading Channels

Figures 9 and 10 are similar to figures 7 and 8, respectively, except that in this section it is assumed an uncorrelated Rayleigh fading channel. Notice that the *PHY mode 5* (16QAM with $R_c=1/2$) has a better performance than the *PHY mode 2* (BPSK with $R_c=3/4$) and *PHY mode* 4 (QPSK with $R_c=3/4$). This interesting characteristic is due to the high coding gain allowed on channels where the Rayleigh multipath fading is temporally independent at symbol level, as postulated in this item. *PHY mode 7* (64QAM with $R_c=2/3$) has a better performance in relation to the *PHY mode 6* (16QAM with $R_c=3/4$) since the higher coding gain overwhelm (in the assumed channel model) the greater noise immunity of 16QAM in relation to the 64QAM signaling scheme. The results shown in Fig. 9 indicate a different interrelation between maximum performance and the PHY mode, since the correlated fading channel assumed in Fig. 8 decreases the net effect of coding gain due to lack of temporal and frequency diversity.

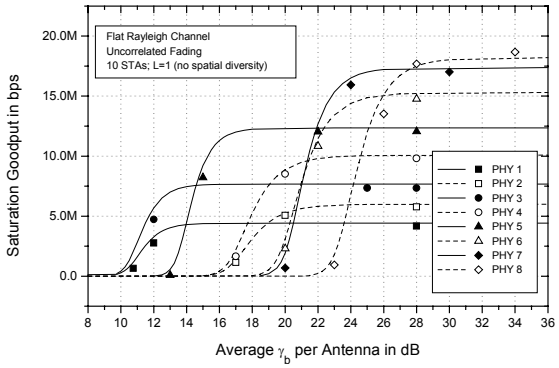

Figure 9. Goodput in bps versus the average SINR per bit.

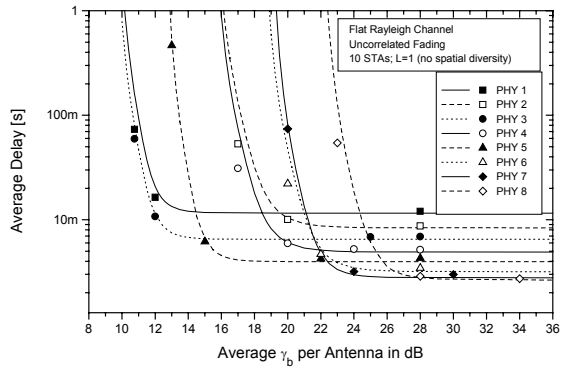

Figure 10. Average delay in seconds versus the average SINR per bit.

IX. CONCLUSIONS

In this paper, we have derived and validated a joint MAC and PHY cross-layer model that can be confidentially used to estimate first order results for the goodput and the delay of IEEE 802.11a ad hoc networks operating simultaneously under the BA and RTS/CTS MAC protocols. We have considered the following environments: *(1)* a flat fading Rayleigh channel that is uncorrelated at symbol level and independent across the OFDM carriers; *(2)* a flat fading Rayleigh channel that is correlated at symbol level and dependent across the OFDM carriers.

REFERENCES

[1] B. P. Crow et al, "IEEE 802.11 wireless local area networks," *IEEE Communications Magazine*, vol. 35, no. 9, pp. 116-126, Sept. 1997.

[2] G. Bianchi, "Performance Analysis of the IEEE 802.11 Distributed coordination function," *IEEE Journal on Selected Areas of Communications*, vol. 18, no. 3, pp. 535-547, March 2000.

[3] J. W. Robinson and J. W. and Randhawa, "Saturation throughput analysis of IEEE 802.11e enhanced distributed coordination function," *IEEE J. on Select. Areas on Communications*, vol. 22, no. 5, pp. 917-928, June 2004.

[4] S. D. Qiao, S. Choi and K. G Shin, "Goodput analyzes and link adaptation for the IEEE 802.11a wireless LANs," *IEEE Trans. Mobile Comp.*, pp. 278-292, 2002.

[5] R. P. F. Hoefel. "A Cross-Layer saturation goodput analysis for IEEE 802.11a networks", *Proc. of IEEE Vehicular Technology Conference 2005-Spring (IEEE VTC 2005-Spring)*, Stockholm, 2005

[6] R. P. F. Hoefel. "Goodput and delay analysis of IEEE 802.11a networks over block fading channels", *Proc. of IEEE Consumer Communication and Networking Conference 2006 (IEEE CCNC 2006),* Las Vegas*,* 2006.

[7] M. S. Gast, *802.11 Wireless Networks*, Sebastopol, CA: O'Reilly, 2005.

[8] IEEE 802.11a, "Part 11: Wireless LAN Medium Access Control (MAC) and Physical Layer (PHY) Specification – Amendment 1: High-speed Physical Layer in the 5 GHz band, supplemented to IEEE 802.11 standard", New Jersey, NY: IEEE Press, Sept. 1999.

[9] J. Conan, "The weight spectra of some short low-rate convolutional codes," *IEEE Transactions on Communications*, vol. 32, pp. 1050-1053, Sept. 1984.

[10] D. Haccoun and G. Bégin, "High-rate punctured convolutional codes for Viterbi and Sequential decoding," *IEEE Transactions on Communications*, vol. 37, n. 11, pp. 1113-1120, Nov. 1989.

[11] M. B. Puersley and D. J. Taipale, "Error Probabilities for Spread-Spectrum Packet Radio with Convolutional Codes and Viterbi Decoding," *IEEE Transactions on Communications*, vol. 35, n. 1, pp. 1-12, Jan. 1987.

[12] J. G. Proakis, *Digital Communications*, New York, NY: MacGraw-Hill, 2001.

[13] L. Yang and L. Hanzo, "A recursive algorithm for the error probability evaluation of M-QAM," *IEEE Comunications Letters*, vol. 4, pp. 304-306, Oct. 2000.

[14] W. C. Jakes, *Microwave Mobile Communications,* New York, NY: Wiley, 1974.

Roger Pierre Fabris Hoefel was born in Porto Alegre, Brazil, on July 9, 1965. He received the B.S degree in electrical engineering from Pontific University Catholic, Porto Alegre, Brazil, in 1990, a Master degree in computer science from Federal University of Rio Grande do Sul, Brazil, in 1995, and a doctor degree in electrical engineering from State University of Campinas, Brazil, in 2000.

He is currently the coordinator of Telecommunications Engineering Department at the University La Salle, Canoas, Brazil. His research interests are in the areas of wireless communications, MAC protocols and signal processing.